

Surface Spin Waves in $^3\text{He-A}$, a Probe for Vortex Phenomena in Narrow Gaps

P. J. Hakonen, K. K. Nummilla, J. T. Simola, L. Skrbek,^(a) and G. Mamniashvili^(b)

Low Temperature Laboratory, Helsinki University of Technology, SF-02150 Espoo 15, Finland

(Received 19 August 1986)

We report measurements on a new collective spin-wave mode trapped by the textural boundary layers of $^3\text{He-A}$ within a stack of thin Mylar plates. The surface mode was seen as a new peak in the cw NMR spectrum measured at $H_0=284$ Oe. Rotation of the sample, with Ω orthogonal to the gaps, increased the spectral weight of the surface mode, indicating an increase in the textural boundary layers caused by a counterflow-induced transition. This phenomenon was used to study vortex creation and persistent currents.

PACS numbers: 67.50.Fi

Textures and textural transitions¹ induced by external magnetic field and superflow in narrow channels have been widely studied both theoretically²⁻⁴ and recently also experimentally.^{5,6} By using transverse cw NMR at $H_0=284$ Oe, we have made the first observation of a localized spin-wave mode trapped by the textural boundary layer in $^3\text{He-A}$. This surface mode, similar to a spin wave trapped by the pure $\hat{\mathbf{I}}$ soliton, has been studied theoretically by Bruinsma and Maki.³ Our observations agree well with their calculations. Furthermore, we find that this new spin-wave mode, and the interaction between the $\hat{\mathbf{I}}$ texture and the superflow, provide in $^3\text{He-A}$ a method for studying the creation and pinning of vortices in narrow gaps when the sample is rotated.

Our experimental volume inside the rf coil consists of a stack of 220 Mylar plates, 3.6 μm thick and with a 3×10 mm² area, and a nominal separation of 19 μm . The Mylar sheets are orthogonal to the rotation axis of the cryostat; the static magnetic field \mathbf{H}_0 can be tilted from this axis by an arbitrary angle θ . The experiments were carried out at 33 bars pressure, at $H_0=284$ Oe, and with $\Omega \leq 3$ rad/s.

The order parameter of $^3\text{He-A}$ is a 3×3 matrix $A_{mn} \propto \hat{d}_m(\hat{\Delta}'_n + i\hat{\Delta}''_n)$, where $\hat{\mathbf{d}}$ is a unit vector, perpendicular to the spin quantization axis, and $\hat{\mathbf{I}} = \hat{\Delta}' \times \hat{\Delta}''$ is the direction of the angular momentum of the Cooper pairs. To enable pairing close to the walls, $\hat{\mathbf{I}}$ is oriented along the surface normal. Away from the walls the orientations of $\hat{\mathbf{d}}$ and $\hat{\mathbf{I}}$ are determined by competition between various free-energy contributions¹: the dipolar energy $-\frac{1}{2}g_D(\hat{\mathbf{I}} \cdot \hat{\mathbf{d}})^2$, the magnetic anisotropy energy $\frac{1}{2}g_D \times [(\mathbf{H}/H_c) \cdot \hat{\mathbf{d}}]^2$, the flow energy (if we neglect terms due to the bending of $\hat{\mathbf{I}}$) $-\frac{1}{2}g_D\{[(\mathbf{v}_s - \mathbf{v}_n)/v_0] \cdot \hat{\mathbf{I}}\}^2$, and the gradient energy, which in the case of small gaps is caused by the $\hat{\mathbf{I}}$ vector bend, $\frac{3}{2}g_D\xi_D^2[\hat{\mathbf{I}} \times (\nabla \times \hat{\mathbf{I}})]^2$. Here $H_c \approx 30$ Oe, $v_0 \approx 1$ mm/s, and the dipolar healing length $\xi_D \approx 10$ μm .

The static magnetic field of 284 Oe $\gg H_c$ ensures that $\hat{\mathbf{d}}$ is almost uniform and perpendicular to \mathbf{H}_0 . The $\hat{\mathbf{I}}$ texture between the plates depends crucially on the gap width w and on the liquid flow in the gap.²⁻⁴ Without counterflow there is a critical width $w_c = (\frac{3}{2})^{1/2}\pi\xi_D \approx 30$

μm (when $\theta=0$). When $w < w_c$ the boundary condition dominates stabilizing $\hat{\mathbf{I}}$ uniformly orthogonal to the plates. When $w > w_c$, the $\hat{\mathbf{I}}$ vector between the plates bends towards $\hat{\mathbf{d}}$, and when $w \gg w_c$ the liquid acquires the state of minimum dipolar energy with $\hat{\mathbf{I}} \parallel \hat{\mathbf{d}}$ everywhere except in the dipolar-unlocked boundary layer near the walls.

The transverse NMR absorption frequency of $^3\text{He-A}$ depends on the texture. In large magnetic fields $f=f_0 + (f_L^2/2f_0)\tilde{f}$, where f_0 is the Larmor frequency, f_L is the temperature-dependent longitudinal resonance frequency, and \tilde{f} is a normalized frequency characteristic to the texture. In a uniform $\hat{\mathbf{I}}$ field a uniform spin wave is excited with $\tilde{f}=\cos 2\alpha$; here α is the angle between $\hat{\mathbf{d}}$ and $\hat{\mathbf{I}}$. Nonuniform textures give rise to localized spin-wave modes with \tilde{f} determined by a Schrödinger-type equation.

When $\hat{\mathbf{I}}$ is bending ($w > w_c$) the conditions close to the Mylar surface resemble pure $\hat{\mathbf{I}}$ -vector solitons,⁷ where the dipole energy of the domain wall acts as a one-dimensional potential well localizing at least one spin-wave mode. The gap-confined spin-wave potential has two minima adjacent to the walls and a maximum in the center. The minima, in units of $f_L^2/2f_0$, are equal to $-\cos 2\theta$, and the height of the maximum between depends on the bending of $\hat{\mathbf{I}}$ and thereby on the gap width. Consequently, the frequency of the lowest-lying eigenmode is very sensitive to the gap width in the vicinity of w_c where $\hat{\mathbf{I}}$ starts to bend, but it levels off rapidly to a constant value, when $w > 40$ μm .³

Typical NMR spectra measured in our Mylar stack with \mathbf{H}_0 perpendicular to the gaps are shown in Fig. 1. In case of an ideal stack with all gap widths equal to the nominal 19 μm , $\hat{\mathbf{I}}$ should be uniformly orthogonal to $\hat{\mathbf{d}}$ leading to a single peak at $\tilde{f}=-1$. Instead, we observe three distinct peaks at $\tilde{f}=-0.83, 0.0$, and 1.0 . Rotation of the cryostat has two prominent effects on the spectrum: The peak at $\tilde{f}=-0.83$ broadens, and the intensity of the central peak near the Larmor frequency increases.

The appearance of these three peaks is easily explained. Because of the bending of the Mylar plates, the

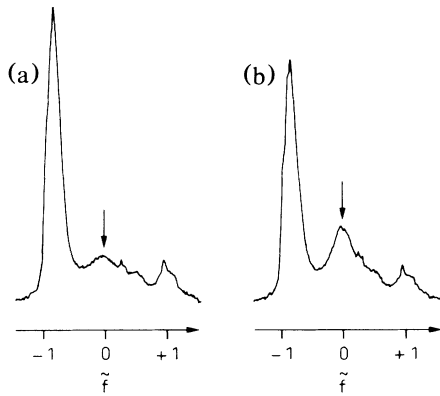


FIG. 1. Measured NMR absorption spectra of ${}^3\text{He-A}$ as a function of $\tilde{f} \equiv (f - f_0)/(f_L/2f_0)$ in a stack of Mylar plates with \mathbf{H}_0 perpendicular to the plates. The line shape (a) in the stationary state and (b) at an angular speed of 0.6 rad/s. The new resonance peak discovered in this work is indicated by arrows. The spectra were recorded at $p = 33$ bars and at $T = 0.73T_c$. The small, sharp spikes originate from unknown nonlinear modes.

gap width varies considerably from one gap to another and even within a single gap. Therefore, w must be considered as a continuous variable ranging from essentially zero (adjacent Mylar plates touching at some point) to a finite value of about $40 \mu\text{m}$. In the presence of this wide distribution of w , a broad NMR absorption line results with maxima at frequencies corresponding to textures that are nearly invariant with respect to w . In our stack there are three such textures: (1) the uniform $\hat{\mathbf{l}} \perp \hat{\mathbf{d}}$ in the regions where $w < w_c$, (2) the uniform $\hat{\mathbf{l}} \parallel \hat{\mathbf{d}}$, where $w \gg w_c$, and (3) the bent- $\hat{\mathbf{l}}$ texture of the textural boundary layer in all the gaps with $w > w_c$.

Figure 2 illustrates this idea more quantitatively. The lower frame shows the schematic $\tilde{f}(w/w_c)$ dependences for the spin-wave modes most strongly coupled to our uniform rf excitation. In the gaps narrower than w_c , $\hat{\mathbf{l}}$ is uniformly orthogonal to $\hat{\mathbf{d}}$ and only the uniform spin wave ("-" mode) in the dipole-unlocked medium is excited, with $\tilde{f}_- = -1$ independent of w . In wider gaps this mode develops gradually into the localized surface mode (SU) with $\tilde{f}_{\text{SU}} \rightarrow 0.12$.³ The second mode ("+" mode) shown in Fig. 2, and discussed by Fetter,⁴ has a twofold character. When $w < w_c$ this mode is nonuniform and dipole unlocked, but above w_c it develops gradually into the uniform spin wave of bulk, dipole-locked ${}^3\text{He-A}$.

Averaging the \tilde{f}_- , \tilde{f}_{SU} , and \tilde{f}_+ branches over the gap-width distribution of our stack produces the spectrum shown in the upper frame. This should be compared with the measured spectra of Fig. 1. A clear discrepancy—irrelevant, however, to the identification of the peaks—is that the observed $\tilde{f}_- = -0.83$ is higher than -1 . A similar feature was seen in earlier experiments on the negative NMR shift in ${}^3\text{He-A}$.⁹ We do not

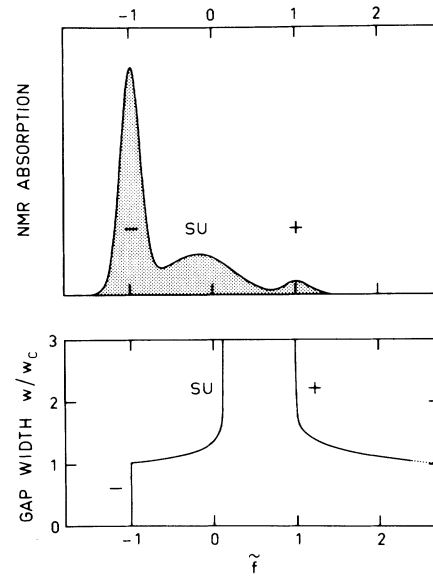


FIG. 2. NMR response of ${}^3\text{He-A}$ in a stack of plates with variable gap width w . The lower frame shows the spin-wave frequencies vs w when \mathbf{H}_0 is orthogonal to the gaps. The spin-wave modes shown are the ones most strongly coupled to the uniform rf excitation: the uniform, dipole-unlocked mode ("-" mode); the surface mode (SU); the uniform, dipole-locked mode ("+" mode). The spectrum in the upper frame results from averaging these modes over the estimated gap distribution (Ref. 8). Most of the (+)-mode intensity is from two large gaps ($w = 19\text{--}100 \mu\text{m}$) outside the Mylar stack. Inside the stack, w is assumed to be uniformly distributed over the range $0\text{--}43 \mu\text{m}$.

know the reason for this discrepancy. The average $\langle \theta \rangle \leq 5^\circ$ due to the nonideal geometry is too small to account for this effect. On the other hand, we believe that our (+)-mode peak is exactly at the frequency of the uniform, dipole-locked spin wave, $\tilde{f}_+ = 1.0$, because we had some bulk volume outside the stack, and because in smaller gaps \tilde{f}_+ is a very steep function of w , leading to a shallow background rather than to a peak. Therefore, we can use the frequency shift $f_+ - f_0 = 28.2(1 - T/T_c)/[1 + 1.93(1 - T/T_c)]$ kHz as our thermometer.^{7,11}

To verify our identification of the new NMR peak we studied its frequency as a function of the tilting angle θ between \mathbf{H}_0 and the gap normal. The result, shown in Fig. 3, is in good agreement with the calculated³ eigenfrequency $\tilde{f}_{\text{SU}}(\theta)$. The temperature dependence of \tilde{f}_{SU} , also shown in Fig. 3, resembles that for spin waves localized by composite solitons observed in open geometry.⁹ Frozen-in $\hat{\mathbf{l}}$ solitons, forced by reversed $\hat{\mathbf{l}}$ orientation at opposing walls in some of the largest gaps, could as well produce an additional absorption maximum, but at a frequency between the SU and + modes. The extra structure between these modes in the measured spectra of Fig. 1 may originate from such solitons.

The counterflow $\mathbf{v}_s - \mathbf{v}_n$, created by rotation of the

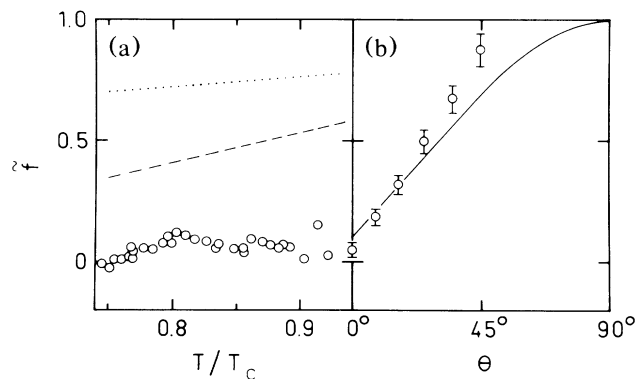


FIG. 3. (a) The normalized frequency shift $\tilde{f}_{\text{SU}} = (f_{\text{SU}} - f_0)/(f_0^2/2f_0)$ for the surface spin-wave (SU) mode vs the reduced temperature. The dotted and dashed lines depict the measured frequencies of the spin waves localized by composite solitons and by continuous A -phase vortices, respectively (Ref. 11). (b) \tilde{f}_{SU} vs the tilting angle θ at $T = 0.78T_c$; the solid line is the calculated dependence (Ref. 3). The error bars grow for larger θ because of the increasing overlap of the SU and (+)-mode peaks.

cryostat, increases the intensity of the surface mode I_{SU} . The frequency \tilde{f}_{SU} also changes with I_{SU} but only slightly, resulting in a maximum change of 0.04 at 0.6 rad/s (see Fig. 1). The primary effect of counterflow is to bend the $\hat{\mathbf{I}}$ vector into the plane of $\mathbf{v}_s - \mathbf{v}_n$, which can induce a textural transition in an $\hat{\mathbf{I}}$ field initially orthogonal to $\mathbf{v}_s - \mathbf{v}_n$.² The critical flow velocity for this transition within a slab geometry is $v_F \approx 0.5h/(2m_3w)$.² For our nominal 19- μm gap width v_F is 0.15 cm/s. We interpret the effects of rotation as being a result of this counterflow-induced Fréedericksz transition⁵ in those parts of the gaps where $w \lesssim w_c$ but $|v_s - v_n|$ is large. The transition increases the surface covered by the textural boundary layers leaving their structure essentially unchanged, thus changing the weight of the mode but not its frequency.

Because of the sensitivity of I_{SU} to the counterflow we could use the NMR spectra measured during rotation to study the vorticity created in the gaps at angular velocities exceeding 0.6 rad/s. We found that I_{SU} depends on the rotational history of the $^3\text{He-A}$ sample. Figure 4 displays the relative absorption $I_{\text{SU}}/I_{\text{tot}}$ vs Ω when the speed of rotation is first increased to 1.8 rad/s, starting from an essentially vortex-free state after cooldown at rest, and then reduced to zero. The shape of the measured hysteresis loop is independent of the sense of rotation.

We see from Fig. 4 that I_{SU} begins to increase as the bending transition starts to occur when $\Omega_F \approx 0.2$ rad/s is exceeded; the initial increase in the absorption is reversible up to about 0.5 rad/s. Above this speed the increase is saturated and the effect is no longer totally reversible, which is a result of the creation of vortices producing a

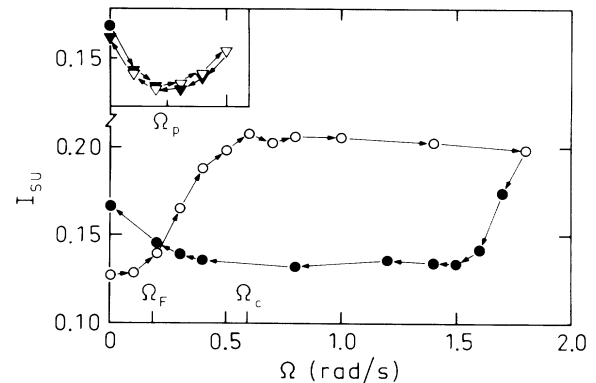


FIG. 4. Observed hysteresis in the relative NMR absorption of the new surface spin-wave mode vs the angular velocity of the cryostat; open circles and filled circles refer to acceleration and deceleration, respectively. When the speed was varied between 0 and 0.5 rad/s after the hysteresis loop had been traversed, the reversible branch with a clear minimum was obtained as shown in the inset (open and filled triangles). The measuring time at each successive speed was 4 min. \mathbf{H}_0 was oriented perpendicular to the plates.

finite \mathbf{v}_s when $\Omega > \Omega_c \approx 0.5-0.6$ rad/s. This limits the counterflow in the peripheral parts of the gaps to 3 mm/s, a value close to the critical velocity observed by Gammel, Ho, and Reppy¹⁰ in $^3\text{He-A}$ intermixed with SiC powder of 25- μm particle size, but an order of magnitude larger than the critical velocity 0.3 mm/s required for the creation of continuous vortices in an open cylinder.¹¹ At speeds above 0.6 rad/s, I_{SU} stays roughly constant.

When the angular velocity is decreased, the counterflow is reduced rapidly because of redistribution of the existing vorticity and the rotation-induced increase in I_{SU} disappears after a reduction of Ω by 0.3 rad/s. During further deceleration I_{SU} stays at the level it had prior to rotation. Below $\Omega = 0.3$ rad/s the absorption begins to grow again and stays at an increased level when the rotation of the cryostat is stopped. Subsequent acceleration from rest decreases I_{SU} and, up to 0.5 rad/s, the reversible parabola shown in the inset of Fig. 4 results.

From the reversible parabola in Fig. 4 we can infer that the counterflow vanishes, i.e., $\mathbf{v}_s \approx \mathbf{v}_n$ macroscopically, at $\Omega_p \approx 0.25$ rad/s. This implies the presence of a persistent current supported by the vortices pinned in the stack.¹² A persistent current in $^3\text{He-A}$ in a torus has been seen in the experiments of Gammel, Ho, and Reppy.¹⁰ Our data show two features that differ from their results: (1) The critical angular velocity for vortex creation Ω_c is approximately twice the Ω_p corresponding to the maximal persistent current, and (2) the fact that I_{SU} stays small during deceleration indicates that the vortices present do not support a reversed rotational counterflow but adjust $\mathbf{v}_s \approx \mathbf{v}_n$ macroscopically. In the experiment of Ref. 10 the maximal Ω_p was equal to Ω_c

and reversed counterflows corresponding to full Ω_c were detected.¹³ These two differences are presumably interrelated and they are associated with the different geometries of the pinning medium.

Rotation also broadens the main NMR line at \tilde{f}_- . This broadening, normalized by the increase in the angular velocity, was $\Delta\Gamma/\Delta\Omega = 110 \pm 30$ in the absence of macroscopic counterflow. A similar broadening observed in the bulk *A*-phase NMR experiments¹¹ arises from the scattering of spin waves from the soft vortex cores. The broadening seen now is two times larger. Also, the critical velocity for vortex creation, being an order of magnitude larger now, indicates that vortices in the narrow gaps differ from vortices in the bulk liquid.

In conclusion, we have found a novel resonance in the NMR spectrum of ³He-*A* in a parallel-plate geometry. The new NMR line is a result of collective surface spin waves in the bent- $\hat{1}$ texture between the plates. Counterflow, induced by rotation, increases the weight I_{SU} of this mode, indicating a counterflow-induced Fréedericksz transition in some parts of the narrow gaps. From the hysteresis loop of $I_{SU}(\Omega)$ we obtain the critical angular speed $\Omega_c = 0.6$ rad/s for vortex formation, as well as the angular velocity $\Omega_p = 0.25$ rad/s of persistent rotational motion supported by remanent vorticity when the cryostat is brought to rest.

It is a pleasure to thank I. Fomin, C.-R. Hu, J. R. Hook, G. A. Kharadze, O. V. Lounasmaa, M. M. Salomaa, and G. E. Volovik for useful discussions. This work, part of the ROTA project, was financially supported by the Academy of Finland and by the Academy of Sciences of the U.S.S.R. The receipt of a scholarship from the Emil Aaltonen Foundation is gratefully acknowledged by one of us (K.K.N.).

^(a)Permanent address: Institute of Physics, Czechoslovak Academy of Science, 18040 Prague 8, Czechoslovakia.

^(b)Permanent address: Institute of Physics, Georgian Academy of Sciences, 380077 Tbilisi, U.S.S.R.

¹See, e.g., D. M. Lee and R. C. Richardson, in *The Physics of Liquid and Solid Helium, Part II*, edited by K. H. Bennemann and J. B. Ketterson (Wiley, New York, 1978), pp. 337–342.

²P. G. De Gennes and D. Rainer, *Phys. Lett.* **46A**, 429 (1974); A. L. Fetter, *Phys. Rev. B* **14**, 2801 (1976), and **15**, 1350 (1977); C.-R. Hu, *Phys. Rev. B* **20**, 276 (1979); T. E. Ham and C.-R. Hu, *J. Low Temp. Phys.* **40**, 31 (1980).

³R. Bruinsma and K. Maki, *J. Low Temp. Phys.* **34**, 343 (1979).

⁴A. L. Fetter, in *Quantum Fluids and Solids—1983*, edited by E. D. Adams and G. G. Ihas, AIP Conference Proceedings No. 103 (American Institute of Physics, New York, 1983), p. 229.

⁵J. R. Hook, A. D. Eastop, E. Faraj, S. G. Gould, and H. E. Hall, *Phys. Rev. Lett.* **57**, 1749 (1986).

⁶D. M. Bates, S. N. Ytterboe, C. M. Gould, and H. M. Bozler, *J. Low Temp. Phys.* **62**, 143 (1986).

⁷K. Maki and P. Kumar, *Phys. Rev. B* **16**, 174 (1977).

⁸To account for spin diffusion the averaged spectrum is convoluted with Gaussians giving appropriate linewidths [P. J. Hakonen, O. T. Ikkala, S. T. Islander, O. V. Lounasmaa, and G. E. Volovik, *J. Low Temp. Phys.* **53**, 425 (1983); P. J. Hakonen, M. Krusius, and H. K. Seppälä, *J. Low Temp. Phys.* **60**, 187 (1985)] for the uniform and localized spin-wave modes. The $\tilde{f}_{SU}(w)$ relation shown in Fig. 2 is from Ref. 3 and $\tilde{f}_+(w)$ is a smooth interpolation between $\tilde{f} \approx -1 + 3(w_c/w)^2$ for small w (Ref. 4), and $\tilde{f} = 1$ for large w . When $w < w_c$ the $+$ mode has no overlap with our uniform rf excitation and the $-$ mode exhausts the spectrum, whereas in gaps wider than w_c we estimate the relative weights of the SU and $+$ modes by w_c/w and $1 - w_c/w$, respectively.

⁹A. I. Ahonen, T. Haavasoja, M. T. Haikala, M. Krusius, and M. A. Paalanen, *Phys. Lett.* **55A**, 157 (1975); A. I. Ahonen, M. A. Paalanen, and M. Krusius, *J. Low Temp. Phys.* **25**, 421 (1976).

¹⁰P. L. Gammel, T.-L. Ho, and J. D. Reppy, *Phys. Rev. Lett.* **55**, 2708 (1985).

¹¹Hakonen *et al.*, Ref. 8; Hakonen, Krusius, and Seppälä, Ref. 8.

¹²In typical persistent-current measurements the experimental volumes are multiply connected. The gaps in our Mylar stack are simply connected by construction, but bending of the plates may have changed this ideal situation.

¹³In general, the use of powder of small grain size in persistent-current experiments leads to $\Omega_p = \Omega_c$ and to a symmetric hysteresis loop $|\Omega_s - \Omega_n| \leq \Omega_c$. This is valid in ³He-*B* and in ³He-*A* as well as in He II; see Ref. 10, and J. P. Pekola, J. T. Simola, K. K. Nummilla, O. V. Lounasmaa, and R. E. Packard, *Phys. Rev. Lett.* **53**, 70 (1984), and references therein.